J. Fluid Mech. (1973), *vol.* 59, *part* 3, *pp.* 493–511
Printed in Great Britain

Nonlinear streaming effects associated with oscillating cylinders

By A. BERTELSEN,

Department of Physics, University of Bergen, Norway

A. SVARDAL AND S. TJØTTA

Department of Applied Mathematics, University of Bergen, Norway

(Received 17 October 1972 and in revised form 6 April 1973)

This paper deals with nonlinear streaming effects associated with oscillatory motion in a viscous fluid. A previous theory by Holtsmark *et al.* (1954) for the streaming near a circular cylinder in an incompressible fluid of infinite extent is reconsidered and used to obtain new numerical results, which are compared with earlier observations. The regime of validity of this theory is considered. The condition to be satisfied by the Reynolds number is found to be less stringent than was previously supposed.

The more recent theory by Wang (1968) based on the outer–inner expansion technique is discussed and corrected with the Stokes drift.

The case of an incompressible fluid enclosed between two coaxial cylinders, one of which is oscillating, is considered in detail. New theoretical and experimental results are given for various values of the parameters involved (Reynolds number, amplitude and cylinder radii).

1. Introduction

The boundary-layer flow (acoustic streaming) induced by an oscillating cylinder is studied theoretically and experimentally. First, we consider the two-dimensional flow occurring near a fixed solid cylinder in an oscillating viscous and incompressible fluid of infinite extent. Since incompressibility is assumed, this flow is the same as that obtained by allowing the cylinder to oscillate in an otherwise quiescent fluid, when referred to an oscillating co-ordinate system fixed to the cylinder. (The vorticity equation and the boundary condition are the same in the two cases.) Taking into account the Stokes drift† (see § 6), it is also proved that the Lagrangian-mean flow is the same, within our approximations, whether an oscillating or a fixed co-ordinate system is used. (See Skavlem & Tjøtta (1955) for a proof to the second order of approximation and Fjæra (1970) for higher order approximations.) This is an important property of the flow, as all experimental observations near an oscillating cylinder refer to a fixed co-ordinate system.

Further, the flow is similar to the one observed in the case of a standing sound

† This drift is frequently called the 'velocity transform' in the acoustic literature.

wave interacting with the same cylinder, provided that the wavelength is large compared with the cylinder radius and that the acoustic Mach number is much smaller than one. Generally, this boundary-layer flow depends on the cylinder radius a, the frequency ω, the amplitude of oscillations and the kinematic viscosity ν. The important parameters are $M = a(\omega/\nu)^{\frac{1}{2}}$, $\epsilon = s/a$, $R_s = \epsilon^2 M^2$ and $\bar{R} = R_s(L_r/a)^2$, where L_r is a characteristic distance for changes in the flow vorticity $\nabla^2\psi_s$ in the radial direction. In recent years the problem has been studied theoretically by several authors using the outer–inner expansion technique (for a review, see Riley 1967).† However, in these works there are few quantitative comparisons with experiments.‡

For the one-cylinder model we present new numerical results based on the theory by Holtsmark *et al.* (1954) for $R_s \ll 1$, and compare these with some earlier experimental observations by Holtsmark *et al.* (1954). The regime of validity of the theory is discussed. In particular, we find that the condition $R_s \ll 1$ can be relaxed to $\bar{R} \ll 1$. We also add some comments on the more recent theory by Wang (1968) based on the outer–inner expansion technique. The theory is corrected with the Stokes drift, and its regime of validity is discussed. Finally, the important case $R_s \gg 1$ is discussed briefly.

Second, the flow of an incompressible viscous fluid enclosed between two coaxial circular cylinders, one of which is oscillating, is also considered. Here $R_s \lesssim 1$. A previous theory by Skavlem & Tjøtta (1955) valid for $A \gg a$ (A is the radius of outer cylinder) is extended to cover arbitrary values of the ratio A/a. New numerical results are given and compared with a series of new experimental observations, as well as with some earlier observations by Olsen (1956) near the inner cylinder.

The present paper is the first of two treating this streaming problem. A second paper by Bertelsen will report on further observations for the case $R_s \gg 1$.

2. Basic equations

For the fluid velocity $\mathbf{v}$ we put

$$\mathbf{v} = \mathbf{v}_u + \mathbf{v}_s, \tag{1}$$

where u and s refer to the unsteady and steady part respectively. On time averaging we get

$$\langle \mathbf{v} \rangle = \langle \mathbf{v}_s \rangle, \quad \langle \mathbf{v}_u \rangle = 0. \tag{2}$$

The fluid is assumed incompressible. We introduce the stream function

$$\psi = \psi_u + \psi_s \tag{3}$$

and separate the basic vorticity equation into an unsteady and a steady part, giving

$$\nu\nabla^4\psi_u - \partial(\nabla^2\psi_u)/\partial t = \mathbf{v}_u.\nabla\nabla^2\psi_s + \mathbf{v}_s.\nabla\nabla^2\psi_u + [\mathbf{v}_u.\nabla\nabla^2\psi_u]_u, \tag{4}$$

$$\nu\nabla^4\psi_s - \mathbf{v}_s.\nabla\nabla^2\psi_s = \langle \mathbf{v}_u.\nabla\nabla^2\psi_u \rangle, \tag{5}$$

† For earlier works, see the review paper by Nyborg (1965).

‡ The related problem of the forces exerted by a viscous fluid on oscillating cylinders has recently been considered by Williams & Hussey (1972).

where $\nu = \mu/\rho$ is the constant kinematic viscosity coefficient. Equations (4) and (5) are nonlinear. To get solvable equations we now make the following approximations, which will be justified later.

(*a*) We linearize (4), i.e. we neglect the right-hand side of the equation.

(*b*) We neglect the second term on the left-hand side of (5). We get

$$\nu\nabla^4\psi_u - \partial(\nabla^2\psi_u)/\partial t = 0, \tag{6}$$

$$\nu\nabla^4\psi_s = \langle \mathbf{v}_u . \nabla\nabla^2\psi_u \rangle. \tag{7}$$

The solution ψ_u of (6) is taken as a first approximation and is inserted into the right-hand side of (7), thereby giving us a linear equation for ψ_s. Thus we find ψ_s and thereby $\mathbf{v}_s$ in the second approximation.

3. Boundary conditions

One cylinder

We introduce cylindrical co-ordinates (r, θ, z), the z axis being along the axis of the cylinder. For $r \to \infty$ the fluid oscillates perpendicular to the axis of the cylinder in the direction $\theta = 0$ with velocity

$$\mathbf{U} = \mathbf{U}_0 \cos \omega t,$$

where $\mathbf{U}_0$ is a constant vector. The boundary conditions for $\mathbf{v}_u$ become

$$\mathbf{v}_u \begin{cases} \to (U_0 \cos\cos\omega t, -U_0 \sin\cos\omega t, 0) & \text{when} \quad r \to \infty, \\ = 0 \quad \text{when} \quad r = a \quad \text{(no-slip condition).} \end{cases} \tag{8}$$

The boundary conditions for $\mathbf{v}_s$ become

$$\mathbf{v}_s \begin{cases} \to \mathbf{0} & \text{when} \quad r \to \infty, \\ = \mathbf{0} & \text{when} \quad r \to a \quad \text{(no-slip condition).} \end{cases} \tag{9}$$

Two cylinders

We introduce a cylindrical co-ordinate system fixed to the inner cylinder. The outer cylinder is oscillating perpendicular to the cylinder axis in the $\theta = 0$ direction with velocity $\mathbf{U} = \mathbf{U}_0 \cos \omega t$.

For a point on the outer cylinder we have

$$\mathbf{r} = \mathbf{r}_0 + \boldsymbol{\xi},$$

where $\mathbf{r}_0$ is the initial position vector of the point and

$$\boldsymbol{\xi} = \int_0^t \mathbf{U}_0 \cos \omega t \, dt = \frac{\mathbf{U}_0}{\omega} \sin \omega t. \tag{10}$$

The velocity of an arbitrary point on the outer cylinder is given by

$$\begin{aligned} \mathbf{v} &= \mathbf{v}(\mathbf{r}_0 + \boldsymbol{\xi}, t) \\ &= \mathbf{v}(r_0, t) + (\boldsymbol{\xi} . \nabla \mathbf{r})_{r=r_0}, \end{aligned} \tag{11}$$

taking into account the first two terms in a Taylor series.

The first-order (linearized) boundary conditions become

$$\left.\begin{aligned} v_r^{(1)}(A,\theta,t) &= U_0\cos\theta\cos\omega t,\\ v_\theta^{(1)}(A,\theta,t) &= -U_0\sin\theta\cos\omega t,\end{aligned}\right\} \tag{12}$$

and these are the conditions used on the oscillatory velocity $\mathbf{v}_u$.

The 'no-slip' requirement on the cylinders leads to the following second-order boundary conditions:

$$\left.\begin{aligned} v_r^{(2)}(A,\theta,t) &= \{-\boldsymbol{\xi}.\nabla\mathbf{v}^{(1)}\}_{r=A}.\mathbf{e}_r,\\ v_\theta^{(2)}(A,\theta,t) &= \{-\boldsymbol{\xi}.\nabla\mathbf{v}^{(1)}\}_{r=A}.\mathbf{e}_\theta.\end{aligned}\right\} \tag{13}$$

The time averages of these expressions are the conditions we use on the streaming velocity $\mathbf{v}_s$. On the inner cylinder the velocities are zero to all orders of magnitude.

We find

$$\langle v_r^{(2)}(A,\theta,t)\rangle = 0, \quad \langle v_\theta^{(2)}(A,\theta,t)\rangle \neq 0,$$

$$\lim_{A\to\infty}\langle v_\theta^{(2)}(A,\theta,t)\rangle = 0 \quad (v_\theta^{(2)}\to 0 \quad \text{as} \quad a^2/A^2\to 0),$$

in agreement with the results by Skavlem & Tjøtta (1955) for $A \gg a$. (For further details, see appendix.)

4. Solution

One cylinder

We first solve (6) subject to conditions (8). The solution is well known from the work of Holtsmark *et al.* (1954). (See equations (2.07) and (2.11) in their paper.) It has the form

$$\psi_u = F(r)\sin\theta\, e^{-i\omega t} + \text{c.c.}, \tag{14}$$

where $F(r)$ involves Hankel functions and changes significantly through the oscillatory boundary layer, i.e. over a distance $\delta_{AC} = (\nu/\omega)^{\frac{1}{2}}$.

Now ψ_u is inserted into (7), which is easily solved subject to conditions (9). The solution turns out to have the form

$$\psi_s = f(r)\sin 2\theta, \tag{15}$$

where $f(r)$ is given by equation (3.12) in the paper of Holtsmark *et al.* (1954).

The solution (15) corrected with the Stokes drift described in § 6 will form the basis for our numerical results for the one-cylinder case.

Two cylinders

We now first solve (6) subject to conditions (12). The solution is readily obtained, but it is given by a very long expression involving Hankel functions with arguments $r(i\omega/\nu)^{\frac{1}{2}}$ and $a(i\omega/\nu)^{\frac{1}{2}}$. It has the same form as (14), but to make a distinction from the one-cylinder case, we write

$$\psi_u = G(r)\sin\theta\, e^{-i\omega t} + \text{c.c.}, \tag{16}$$

and refer to the appendix for derivation of the solution and further details.

This first-order solution is inserted into the quadratic terms in the streaming equation (7), and the resulting equation is solved using the above-mentioned boundary conditions for the streaming velocity. The solution is given by very complicated integrals which have to be solved numerically. We write

$$\psi_s = g(r)\sin 2\theta, \tag{17}$$

where $g(r)$ is given by (A 9) in the appendix. This solution corrected with Stokes drift described in § 6 forms the basis for our numerical analysis of the two-cylinder case.

A preliminary theoretical report on this case with two cylinders is given by Svardal (1965); our formal solution is the same as his. The numerical approach to the solution, however, differs. The accuracy of Svardal's numerical results is not sufficient to explain the observed effects a little away from the inner cylinder.

Numerical methods

The numerical calculations were carried out on an IBM 360/50 HG computer in double-precision mode. Numerical values of the Hankel functions were obtained from the asymptotic series. Simpson's formula was used in the integrations necessary for obtaining the stream function. The tangential (particle) velocity component was obtained by numerical differentiation of the stream function.

5. Validity of the method used

Let us first consider the one-cylinder case. We assume

$$\delta_{AC} < a, \quad \text{i.e. } M > 1.$$

The solutions of the linearized equation (6) are found to be a good approximation to the unsteady stream function if

$$\epsilon = U_0/\omega a \ll 1, \tag{18}$$

i.e. the oscillating amplitude is much smaller than the cylinder radius. This is known from previous studies (see, for example, Riley 1967) and is also found by inserting into the different terms of (4) the solutions obtained for ψ_u and ψ_s from (6) and (7).

Further, inserting these solutions also into (5), we find that the second term of this equation is of order $\bar{R}$ relative to the first one. Thus the approximation introduced in (7) by neglecting this term can only be justified if

$$\bar{R} = \frac{V_s}{\nu}\frac{L_r^2}{L_\theta} \ll 1. \tag{19}$$

Here V_s is a characteristic value of the θ component of the steady velocity and L_r and L_θ are characteristic distances for changes in the vorticity $\nabla^2\psi_s$ in the r and θ directions respectively.

This, however, presumes that the uniform flow represented by the boundary condition (8) for $r \to \infty$ is reached at $r/a = O(1)$. In other cases we have to consider other approximations (Oseen type; see Riley 1967; Fjæra 1970) away from the

cylinder and base our studies on matching principles. On the other hand, using an Oseen type of approximation uniformly for all $r \geqq a$ leads to no second-order streaming effects, when one takes into account the Stokes drift (see Westervelt 1953).

Schlichting in his model (1932) found $U_0^2/\omega a$ to be a characteristic value of V_s. He further had $L_\theta = a$. Inserting this in (20) we get

$$\bar{R} = \frac{U_0^2}{\omega\nu}\left(\frac{L_r}{a}\right)^2 \ll 1.$$

As $L_r < a$, here too our method is expected to give correct results for

$$R_s = U_0^2/\omega\nu \leqq 1. \tag{20}$$

In practice it seems to predict the streaming correctly at least up to $R_s \simeq 1$; see results in § 8. (Riley (1967) and Wang (1968) give more restricted ranges of validity for this method.)

For $R_s \gg 1$ Stuart (1966) and Riley (1965) have discussed the possibility of an outer steady boundary layer within which the streaming is governed by the full nonlinear Navier–Stokes equations. Its thickness is of order $aR_s^{-\frac{1}{2}}$, which is also obtained by putting $\bar{R} = 1$. Schlichting's inner solution (see § 9) is assumed to be valid near the cylinder and is used to determine the solution for the outer boundary layer. One obtains Schlichting's solution from the one given by Holtsmark *et al.* (1954) by carrying out an expansion in powers of M^{-1} (see Raney, Corelli & Westervelt 1954). It is therefore of interest here to note that $\bar{R} \ll 1$ within Schlichting's boundary layer. In fact we find

$$L_r = \delta_{DC} = O(\delta_{AC}) \ll a,$$

implying that

$$\bar{R} = R_s M^{-2} = \epsilon^2 \ll 1.$$

This indicates that Schlichting's inner solution is a good approximation to the solution near the cylinder, a result that is also supported by our recent measurements (for $R_s \gg 1$, see Bertelsen 1971).

Considering now the case with two cylinders, we find by similar arguments

$$\bar{R} = R_s(L_r/L_\theta)^2 \ll 1 \tag{21}$$

as a condition for using the method described in § 4.

6. Stokes drift

The velocities found so far are the Eulerian velocities $\mathbf{v}^E$. The observed velocities, however, are found by following one particle over some distance for some time and calculating the average velocity, i.e. one observes the average Lagrangian velocity. Therefore, before comparing our theory with experimental results we have to find the Lagrangian velocities $\mathbf{v}_u^L$ and $\mathbf{v}_s^L$ from our previous results. The relations between the Lagrangian and Eulerian velocities are in our approximation

$$\mathbf{v}_u^L = \mathbf{v}_u^E = \mathbf{v}_u, \tag{22}$$

$$\mathbf{v}_s^L = \mathbf{v}_s^E + \langle \int \mathbf{v}_u \, dt \,.\, \nabla \mathbf{v}_u \rangle. \tag{23}$$

Thus the unsteady velocity does not have to be corrected. The steady velocity $\mathbf{v}_s^E$ has to be corrected by a term $\Delta\mathbf{v}_s = \langle\int\mathbf{v}_u\,dt.\nabla\mathbf{v}_u\rangle = -\frac{1}{2}\nabla\times\langle\mathbf{v}_u\times\int\mathbf{v}_u\,dt\rangle$, the Stokes drift or velocity transform. The importance of this term was first pointed out by Stokes (1847) and later by Rayleigh (see Rayleigh 1945). This term has been accounted for by Raney *et al.* (1954) and Skavlem & Tjøtta (1955). For the steady stream functions we get the following relation:

$$\psi_s^L = \psi_s^E + C(r,\theta), \tag{24}$$

where $C(r,\theta)$ is defined by

$$\Delta\mathbf{v}_s = -\nabla\times(C\mathbf{k}),$$

$\mathbf{k}$ being a unit vector in the z direction.

For the case of one cylinder, $C(r,\theta)$ is given by equation (14) in Raney *et al.* (1954), and has the form

$$C(r,\theta) = h(r)\sin 2\theta.$$

This implies that we can write

$$\psi_s^L = f(r)\sin 2\theta + h(r)\sin 2\theta = f^L(r)\sin 2\theta.$$

For the case of two cylinders, $C(r,\theta)$ is given by (A 12) and ψ_s^L by (A 13) in the appendix.

The correction term $C(r,\theta)$ is approximately zero away from the boundaries. Near the boundaries there is a phase shift in the oscillations depending on r and θ, and there the effect of the Stokes drift is significant. It affects the thickness of the steady boundary layers and the values of the steady velocities.

At the outer boundary the effects of the nonlinear boundary condition (cf. (13) *et seq.*) cancel the Stokes drift effects leading to the physically meaningful result that the steady part of the particle velocity (Lagrangian mean velocity) is zero at this boundary.

7. Apparatus and method of observation

The apparatus is much the same as that used by Olsen (1956). However, some modifications and improvements were necessary to enable us to study the streaming for high R_s and to take into account the effects of the outer boundary. A sketch of our apparatus is shown in figure 1.

The inner cylinder is suspended with perlon lines. This cylinder is forced to oscillate sinusoidally by putting the cylinders in a strong, constant magnetic field and supplying the inner cylinder with an alternating current.

The motion of the fluid is made visible by tracing particles and photographed in stroboscopic light synchronized to the frequency of oscillation or the integral part of this.

For $R_s \simeq 0{\cdot}75$ the experiments were performed in air and in a mixture of water and glycerol to give a kinematic viscosity of $0{\cdot}15\,\mathrm{cm}^2/\mathrm{s}$. For the case $R_s \gg 1$ ($R_s \simeq 90$ and 400) the fluid was pentane.

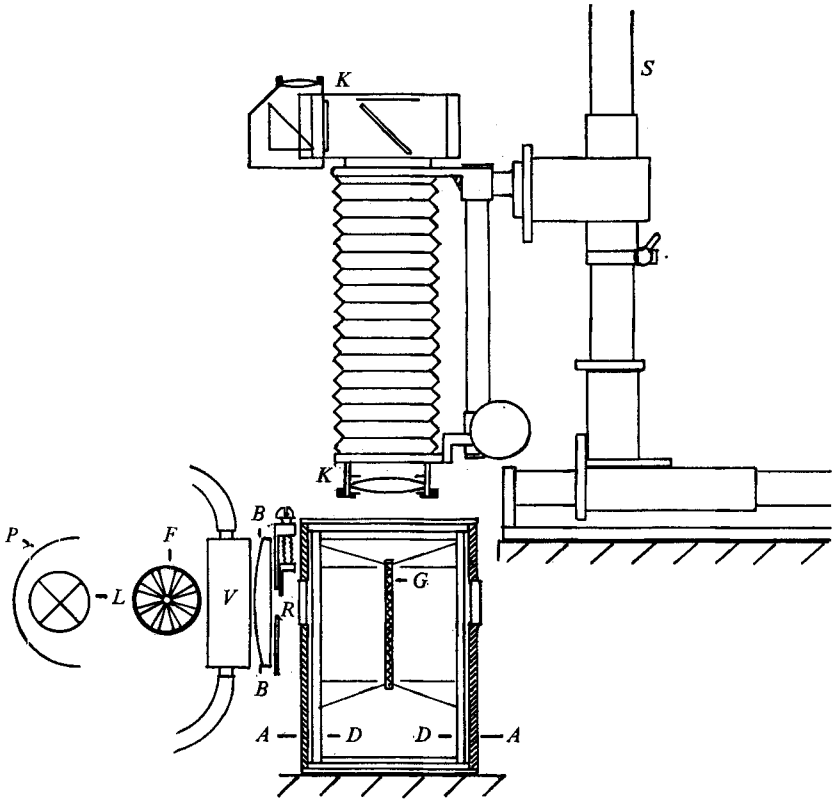

FIGURE 1. Sketch of the apparatus used in the experimental investigation: G, inner oscillating cylinder; A, D, outer cylinder with double walls; P, L, F, B, R, illumination equipment; K, camera with bellow and lens; S, camera tripod.

8. Results and discussions

$R_s \simeq 1$, *one cylinder*

For different values of the cylinder radius a we have computed the thickness δ_{DC} of the inner steady boundary layer defined by $\delta_{DC} = r - a$, where r is the zero point of $f^L(r)$. The results are given by curve I in figure 2, where we also have plotted the experimental values (denoted by circles) found by Holtsmark *et al.* (1954) for the case of a standing sound wave interacting with a cylinder. The agreement between theory and experiment is excellent. The theoretical point $\delta_{DC} = 0{\cdot}068$ cm for $a = 0{\cdot}11$ cm found earlier by Skavlem & Tjøtta (1955) and by Raney *et al.* (1954) fits in with these results. In the experiments ϵ ranges from $\frac{1}{17}$ to $\frac{1}{85}$ so condition (18) holds. Further one typically has $\bar{R}$ or order 10^{-1}, implying that condition (19) also holds. The range of M is from 10 to 50.

To illustrate the importance of the Stokes drift we have plotted (curve II, figure 2) the numerical values for the thickness of the inner steady layer found by Holtsmark *et al.* (1954) without adding the Stokes drift. The curve approaches curve III, representing the numerical value found by Schlichting (1932), whereas curve I approaches curve IV, representing the corrected Schlichting value found by Raney *et al.* (1954).

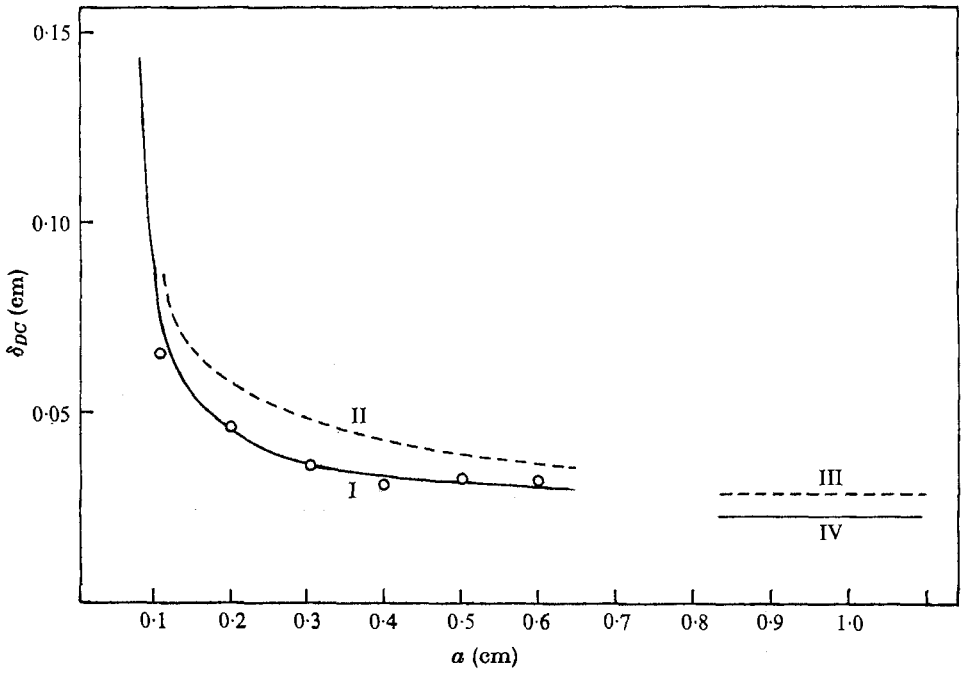

FIGURE 2. Thickness of inner vortex system versus radius of inner cylinder. Frequency $\omega = 2\pi \times 200\ \mathrm{s}^{-1}$, kinematic viscosity $\nu = 0{\cdot}15\ \mathrm{cm}^2/\mathrm{s}$. I, this work; II, Holtsmark *et al.* (1954); III, Schlichting (1932); IV, corrected Schlichting value found by Raney *et al.* (1954). ——, – – –, theory; ○, experiment (Holtsmark *et al.* 1954).

$R_s \lesssim 1$, *two cylinders*

Olsen (1955, 1956) has observed the flow between two coaxial cylinders, the inner one oscillating. The observations are limited to regions $r/a < 3{\cdot}2$ near the inner cylinder. They are referred to a fixed co-ordinate system, but because of the invariance properties of the flow (see introduction), we can make a comparison with the results of our theoretical models. Olsen also has typically $\bar{R}$ of order 10^{-1}. The one-cylinder theory compares favourably with the observations near the inner cylinder ($r/a \lesssim 2,5$), where the outer boundary, for these cylinder radii, has little influence on the streaming. The effect from the Stokes drift, however, is significant and has to be taken into account. It affects the thickness of the inner steady boundary layer. Olsen's observations also fit nicely with the results of figure 2 (curve I).

The two-cylinder theory also leads to good agreement with Olsen's observations $v^L_{s,\theta}$ for the case $A/a = 8$ for $r/a > 2{\cdot}5$, see figure 3. For higher values of A/a his observations seem to be uncertain away from the inner cylinder. For $A/a = 20$ and the other parameters as in figure 3 the theory gives $r_c/a \approx 5{\cdot}0$ for the position of the cores of the outer vortex systems. This is in agreement with the result reported previously by Skavlem & Tjøtta (1955). However, Olsen's observations seem to indicate a much lower value, i.e., $r_c/a \approx 3{\cdot}0$. Skavlem & Tjøtta explain this discrepancy as probably due to inaccuracy in the numerical calculations at this distance from the inner cylinder. Now we believe that the discrepancy is

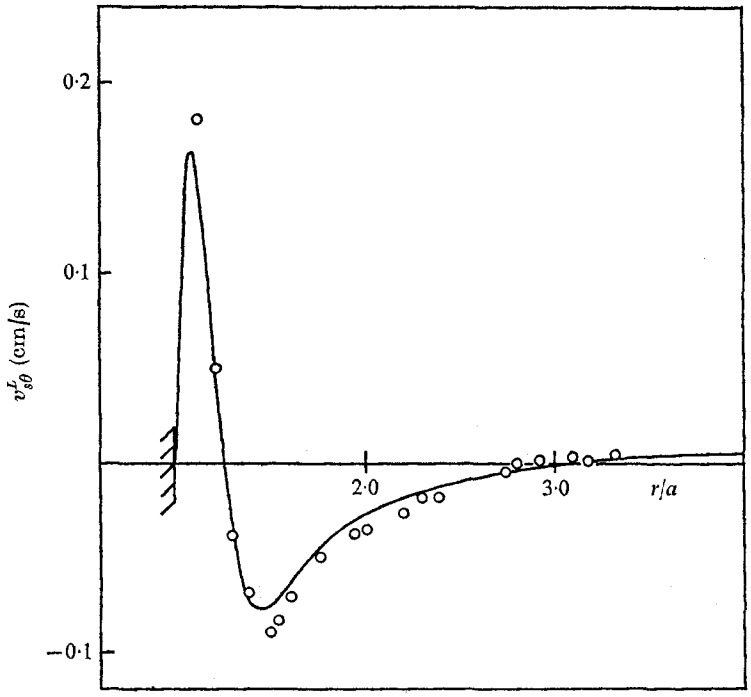

FIGURE 3. Steady part of tangential Lagrangian velocity at $\theta = 45°$, $U_0 = 7{\cdot}4$ cm/s, $\nu = 0{\cdot}15$ cm^2/s, $\omega = 2\pi.200$ s^{-1}, $a = 0{\cdot}11$ cm, $A = 8a$. ——, theory; ○, experimental values (Olsen 1956).

due to the experimental model used by Olsen. His model did not generate two-dimensional motion as was presumed in the theory. Probably the cylindrical enclosure was too short in the direction orthogonal to the plane of motion. It is easy to verify experimentally that shortening the length of the cylindrical enclosure causes the cores of the outer vortex systems to move inwards. Our new observations lead to $r_c/a = 5{\cdot}0 \pm 0{\cdot}2$ for $A/a = 20$, in perfect agreement with theory.

We have been interested in determining the influence of the outer boundary on the steady streaming and examining the limit of validity of the theory. First, the main features of the flow at various radii of outer boundary, all other parameters constant, are shown in figures 4–7 (plates 1–4). A minute experimental investigation of the effect of the outer boundary was carried out by measuring the following quantities for various radii of outer boundary.

(*a*) The thickness of the inner vortex system.

(*b*) The position of the core of the inner vortex system.

(*c*) The position of the core of the outer vortex system.

(*d*) The steady part of the tangential particle velocity at $\theta = 45°$.

Table 1 gives $U_0 \approx 8{\cdot}4$ cm/s $\pm 5\,\%$, $M \approx 9{\cdot}5 \pm 2\,\%$ and $R_s \approx 0{\cdot}75 \pm 8\,\%$.

The results for (*a*), (*c*) and (*d*) compared with corresponding theoretical results are shown in figures 8–12.

The position of the core of the inner vortex system was found to be constant

$a \approx 0{\cdot}147$ cm $\pm 1\,\%$,	$\omega \approx 2\pi \times 100\ \mathrm{s}^{-1} \pm 2\,\%$,
$\nu \approx 0{\cdot}15\ \mathrm{cm}^2/\mathrm{s} \pm 2\,\%$,	$\epsilon \approx \frac{1}{11} \pm 5\,\%$.

TABLE 1. Parameters constant during the investigation

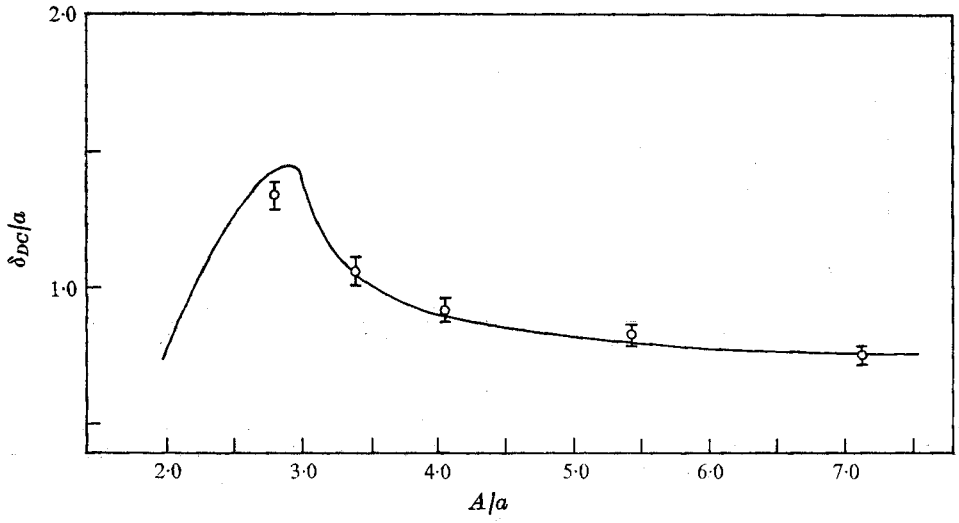

FIGURE 8. Thickness of inner vortex system as function of A/a. The most important parameters are as given in table 1. ——, theory; ○, experiment.

experimentally (within experimental uncertainty) and varies by less than one per cent theoretically for those ratios A/a considered, i.e. 2–15.

Figure 8 shows that the thickness of the inner vortex system is influenced by the outer boundary when $A/a < 5{\cdot}0$, and that the theory describes this dependence very well.

Figure 9 shows the position of the core of the outer vortex system for

$$2{\cdot}0 < A/a < 10{\cdot}0.$$

It is shown to be sensitive to changes of the radius of the outer boundary, and comparison between theory and experiment indicates good agreement.

Figures 10, 11 and 12 show the velocity of the steady streaming for different values of A/a. For the lowest values of A/a we notice an increase in the velocity maximum with decreasing A/a.

We can conclude that our theory predicts results that are in good agreement with observations when $\epsilon \ll 1$ and $\bar{R} \ll 1$. The case $R_s \lesssim 1$ is included in this for $L_r < a$. The Stokes drift has to be introduced to adapt the theoretical results to the experiments.

$$R_s \gg 1$$

For $R_s > 1$ there are to date only a few qualitative experiments by Schlichting (1932) and others. Thus Olsen (1955) has observations for $R_s = 25$, but with large amplitude, $\epsilon = 0{\cdot}7$ and $M = 7$. For these values of R_s and M he finds that the

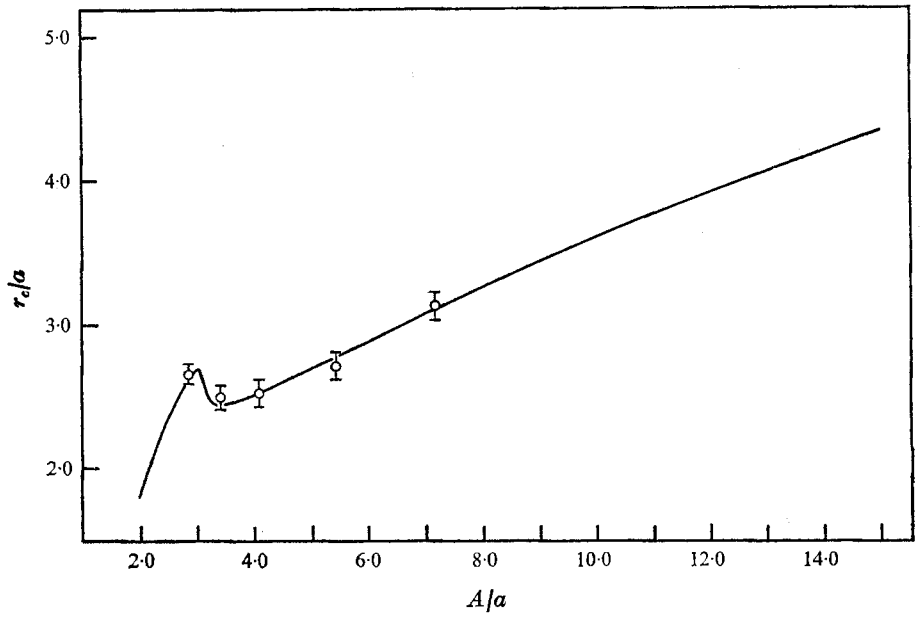

FIGURE 9. Radial position of the core of the outer vortex systems as a function of A/a. Angular position of the core in the first quadrant is $\theta = 45°$. The most important parameters have the values given in table 1. ——, theory; $\overline{\bigcirc}$, experiment.

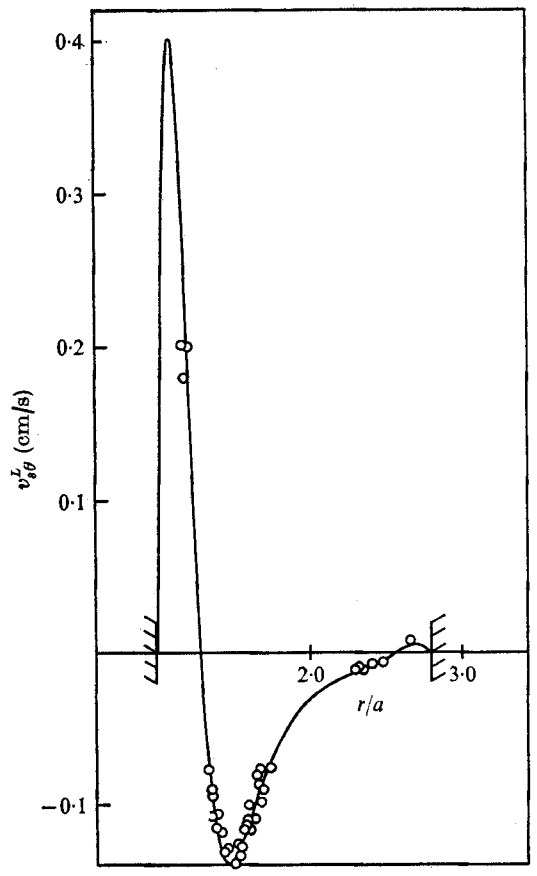

FIGURE 10. Steady part of the tangential Lagrangian velocity at $\theta = 45°$ for $A/a = 2{\cdot}82$. Other important parameters as in table 1. ——, theory; ○, experiment.

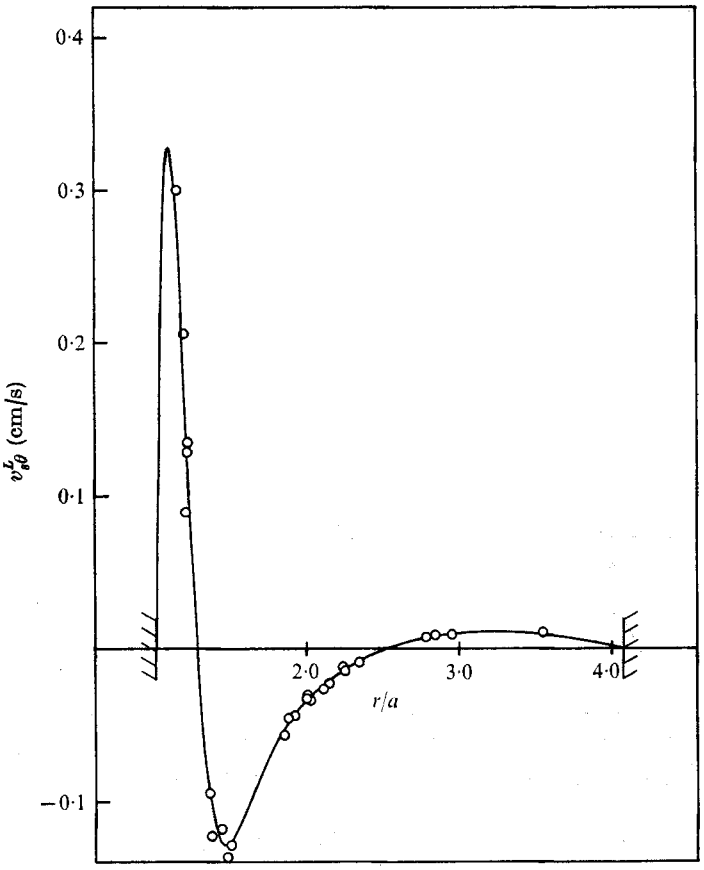

FIGURE 11. Steady part of the tangential Lagrangian velocity at $\theta = 45°$ for $A/a = 4{\cdot}08$. Other important parameters as in table 1. ——, theory; ○, experiment.

thickness of the inner layer decreases slightly with increasing amplitude. For lower values of M, this decrease in thickness with increasing amplitude becomes very strong, according to the observations by Skogen (1951) and by Raney *et al.* (1954).

The theories of Riley (1965), Stuart (1966) and Davidson & Riley (1972) are based on the assumption $R_s \gg 1$. Our experimental set-up allows measurements in this high R_s region. Thus at $R_s = 90$ and $R_s = 400$ a typical outer boundary layer for the steady streaming is established, in qualitative agreement with the theories. Also a strong jet is formed in the direction along the axis of oscillation (see figure 13, plate 5). Further work on this case is in progress and will be reported elsewhere.

9. Wang's theory

Wang (1968) has used outer–inner asymptotic expansions on the same streaming problem. The expansions are valid for large M only. For the inner region a stretched co-ordinate is introduced, defined by $r/a = 1+\eta/M$. The matching of

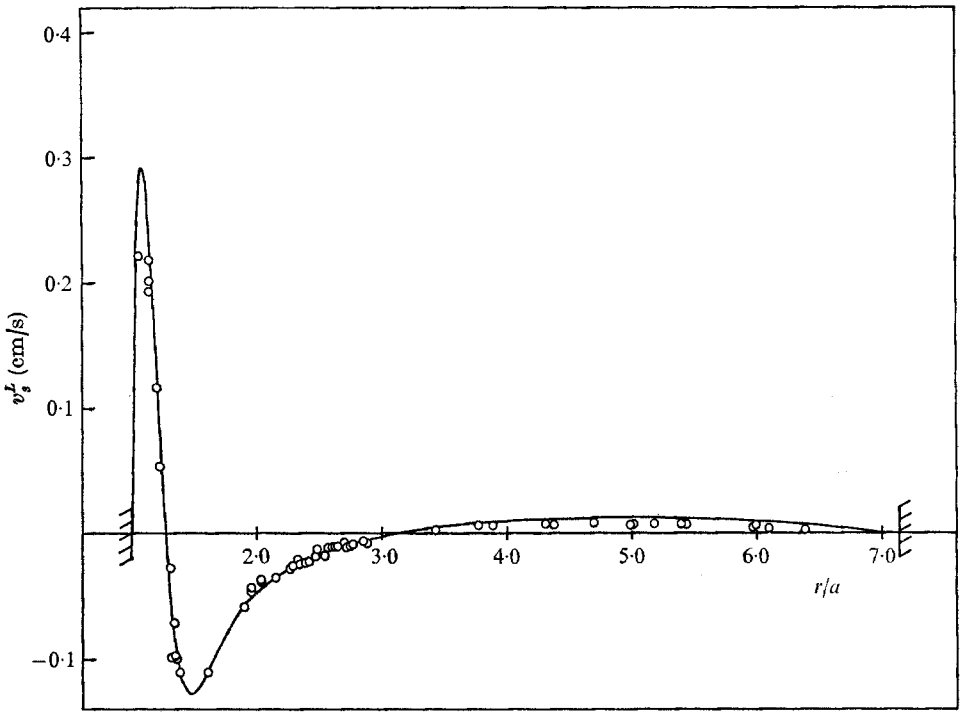

FIGURE 12. Steady part of the tangential Lagrangian velocity at $\theta = 45°$ for $A/a = 7{\cdot}14$. Other important parameters as in table 1. ——, theory; ○, experiment.

an outer and an inner solution results, for instance, in a steady stream function which is uniformly valid. It may be written as

$$\overline{\psi} = \epsilon \sin 2\theta \left\{ \frac{3}{4}\left(\frac{1}{\bar{r}^2} - 1\right) + \frac{1}{M}\left[\frac{13}{2\sqrt{2}} - \frac{1}{2\sqrt{2}} e^{-\eta/\sqrt{2}} \left(12 \cos \frac{\eta}{\sqrt{2}} + 8 \sin \frac{\eta}{\sqrt{2}} + e^{-\eta/\sqrt{2}} \right) - \eta\, e^{-\eta/\sqrt{2}} \sin \frac{\eta}{\sqrt{2}} \right] \right\}, \quad (25)$$

where $\bar{r} = r/a$.

We have here introduced the term $-\epsilon(\eta/M)\, e^{-\eta/\sqrt{2}} \sin(\eta/\sqrt{2}) \sin 2\theta$, which is left out in Wang's solution (the term $Re(-i\eta E)$ from his inner expansion, equation (3.36)).

Let $\overline{\psi} = 0$ for $\eta = \eta_0$. Then $\delta_{DC}/a = \eta_0/M$, and from this Wang has found the values δ_{DC}/a for different values of a (and thereby of M^2). Also his results agree well with the experimental results by Holtsmark *et al.* (1954) (replotted here on figure 2). We note, however, that this agreement is achieved without introducing the correction due to the Stokes drift described in § 6, the magnitude of which is indicated in our figure 2. The observations are for M ranging from 10 to 50. We would not expect Wang's result to be valid for these moderate values of M. We find that the matching leading to (25) is correct to first order in η/M only (v_r matches only to first order). Thus $\eta/M \ll 1$ is presumed in the theory, whereas η/M is as high as 0·8 for $M = 10$.

In fact if we compute the flow field from (25), using the same parameters as in figure 3, we find, for example,

$$\max v_\theta \approx 0{\cdot}25 \text{ cm/s for } r/a \approx 1{\cdot}12, \quad \min v_\theta \approx -0{\cdot}19 \text{ cm/s} \quad \text{for} \quad r/a \approx 1{\cdot}54.$$

This does not agree with observations (see figure 3).

We have computed the Stokes drift correction to Wang's steady solution, using his unsteady solutions. His inner solution leads to the following correction in the stream function:

$$\Delta\overline{\psi}_i = \frac{\epsilon}{2\sqrt{2}}\frac{1}{M}\sin 2\theta\left[e^{-\eta/\sqrt{2}}\left(4\frac{\eta}{\sqrt{2}}\sin\frac{\eta}{\sqrt{2}}+4\cos\frac{\eta}{\sqrt{2}}-2e^{-\eta/\sqrt{2}}\right)-2\right]+O(M^{-2}), \tag{26}$$

and his outer solution leads to

$$\Delta\overline{\psi}_y = -\frac{\epsilon}{Mr^2\sqrt{2}}\sin 2\theta + O(M^{-2}). \tag{27}$$

We note that

$$\lim_{\eta\to\infty}\Delta\overline{\psi}_i = \lim_{\eta\to 1}\Delta\overline{\psi}_y = -\frac{1}{M\sqrt{2}},$$

and uniformly valid corrected steady solution (in Wang's approximation scheme) is readily obtained:

$$\overline{\psi}_c = \epsilon\sin 2\theta\left\{\left(\frac{3}{4}-\frac{1}{M\sqrt{2}}\right)\left(\frac{1}{\bar{r}^2}-1\right)+\frac{1}{M}\left[\frac{11}{2\sqrt{2}}-\frac{1}{2\sqrt{2}}e^{-\eta/\sqrt{2}}\right.\right.$$
$$\left.\left.\times\left(8\sin\frac{\eta}{\sqrt{2}}-8\cos\frac{\eta}{\sqrt{2}}+3e^{-\eta/\sqrt{2}}\right)\right]\right\}+O(\epsilon M^{-2}). \tag{28}$$

Putting $\bar{r} = 1+\eta/M$, and neglecting consistently terms of order ϵ/M^2 (note such terms are not accounted for in the inner expansion up to our order), we get

$$\overline{\psi}_c = \epsilon M^{-1}\sin 2\theta\left\{-\tfrac{3}{2}\eta+\frac{11}{2\sqrt{2}}-\frac{1}{2\sqrt{2}}e^{-\eta/\sqrt{2}}\left(8\sin\frac{\eta}{\sqrt{2}}+8\cos\frac{\eta}{\sqrt{2}}+3e^{-\eta/\sqrt{2}}\right)\right\}, \tag{29}$$

which is Schlichting's inner solution corrected with the Stokes drift (cf. Raney *et al.* (1954) and our figure 2).

Now

$$\overline{\psi}_c = 0$$

leads to $\eta \approx 2{\cdot}083$, independent of M (but valid only for $M \gg 1$, or in practice $M \gg 10$ to give $\eta/M \ll 1$). In this approximation

$$\delta_{DC}/a \approx 2{\cdot}083/M$$

and

$$\delta_{DC}/\delta_{AC} \approx 2{\cdot}083.$$

We conclude that Wang's method, when one matches to the first order only, should give Schlichting's value for the thickness of the steady boundary layer. The asymptotic expansions in $1/M$, when matched to higher order in η/M, may, however, be used for moderate values of M (about 50), but the convergence seems to be slow, and it cannot, with the present stretching $\bar{r} = 1+\eta/M$, explain the strong increase in δ_{DC} with decreasing a (and thereby M) as observed for moderate

M. Matching to second order should compare with including terms $O(1/M^2)$ in the expansion of the theory by Holtsmark *et al.* (1954), and which are given by Raney *et al.* (1954).

The authors are grateful to L. E. Engevik and H. Hobæk for most valuable discussions on this work.

Appendix

First-order solution (two cylinders)

We define Φ by

$$\nabla^2\psi_u = \Phi \tag{A 1}$$

and write (8) in the form

$$\left(\nabla^2 - \frac{1}{\nu}\frac{\partial}{\partial t}\right)\Phi = 0, \tag{A 2}$$

with

$$\Phi = R(r)\sin\theta\, e^{-i\omega t} + \text{c.c.}$$

Equation (A 2) leads to a Bessel equation in $R(mr)$, where $m = (i\omega/\nu)^{\frac{1}{2}}$. By substituting its solutions for Φ expressed by Hankel functions $H_1^{(1)}(mr)$ and $H_1^{(2)}(mr)$ in (A 1) and assuming

$$\psi_u = G(r)\sin\theta\, e^{-i\omega t} + \text{c.c.},$$

we obtain

$$G''(r) + \frac{1}{r}G'(r) - \frac{1}{r^2}G(r) = B_1 H_1^{(1)}(mr) + B_2 H_1^{(2)}(mr),$$

which can be solved by elementary methods. The first-order solution ψ_u can be written as

$$\psi_u(r,\theta,t) = \left\{\frac{B_1}{2m}\left[r(H_0^{(1)}(mr) - H_0^{(1)}(mr)) + \frac{1}{r}(H_2^{(1)}(mr)\,a^2 - r^2 H_2^{(1)}(mr))\right]\right.$$
$$\left. + \frac{B_2}{2m}\left[r(a^2 H_0^{(2)}(ma) - H_0^{(2)}(mr)) + \frac{1}{r}(a^2 H_2^{(2)}(ma) - r^2 H_2^{(2)}(mr))\right]\right\}$$
$$\times \sin\theta \exp(-i\omega t) + \text{c.c.}, \tag{A 3}$$

where

$$\frac{B_1}{2m} = -\frac{U_0}{N}[a^2 H_2^{(2)}(ma) - A^2 H_2^{(2)}(mA)],$$

$$\frac{B_2}{2m} = \frac{U_0}{N}[a^2 H_2^{(1)}(ma) - A^2 H_2^{(2)}(mA)],$$

$$N = [H_0^{(1)}(ma) - H_0^{(1)}(mA)][a^2 H_2^{(2)}(ma) - A^2 H_2^{(2)}(mA)]$$
$$- [H_0^{(2)}(ma) - H_0^{(2)}(mA)][a^2 H_2^{(1)}(ma) - A^2 H_2^{(1)}(mA)],$$

when we take into account the boundary conditions (12).

For the velocity components we obtain

$$v_{u,r} = \text{Re}\,[S(r)\cos\theta\, e^{-i\omega t}] = [S_1(r)\cos\omega t + S_2(r)\sin\omega t]\cos\theta, \tag{A 4}$$

$$S(r) = -\frac{B_1}{2m}\left[H_0^{(1)}(ma) - H_0^{(1)}(mr) + \frac{a^2}{r^2}H_2^{(1)}(ma) - H_2^{(1)}(mr)\right]$$
$$- \frac{B_2}{2m}\left[H_0^{(2)}(ma) - H_0^{(2)}(mr) + \frac{a^2}{r^2}H_2^{(2)}(ma) - H_2^{(2)}(mr)\right],$$

$$v_{u,\theta} = \mathrm{Re}\,[T(r)\sin\theta\, e^{-i\omega t}]$$
$$= [T_1(r)\cos\omega t + T_2(r)\sin\omega t]\sin\theta, \tag{A 5}$$

$$T(r) = \frac{B_1}{2m}\left[H_0^{(1)}(ma) - H_0^{(1)}(mr) - \frac{a^2}{r^2}H_2^{(1)}(ma) + H_2^{(1)}(mr)\right]$$
$$+ \frac{B_2}{2m}\left[H_0^{(2)}(ma) - H_0^{(2)}(mr) - \frac{a^2}{r^2}H_2^{(2)}(ma) + H_2^{(2)}(mr)\right].$$

Second-order solution (two cylinders)

Introducing

$$\left.\begin{aligned} J(mr) &= \frac{B_1}{2m}\frac{H_0^{(1)}(mr)}{U_0}, \quad D = J(ma), \\ K(mr) &= \frac{B_1}{2m}\frac{H_2^{(1)}(mr)}{U_0}, \quad E = K(ma), \\ M(mr) &= \frac{B_2}{2m}\frac{H_0^{(2)}(mr)}{U_0}, \quad F = M(ma), \\ N(mr) &= \frac{B_2}{2m}\frac{H_2^{(2)}(mr)}{U_0}, \quad G = N(ma), \end{aligned}\right\} \tag{A 6}$$

we obtain on substituting the first-order solution in (9)

$$\nu\nabla^4\psi_s = \lambda(r)\sin 2\theta, \tag{A 7}$$
$$\lambda(r) = -\frac{U_0^2\omega}{2\nu}\,\mathrm{Im}\left[(D^*+F^*)(K+N) + 2(J+M)(K^*+N^*) + \frac{a^2}{r^2}(E+G)(J^*+M^*)\right].$$

Putting $\psi_s = g(r)\sin 2\theta,$

we readily obtain

$$g(r) = r^4\left[\frac{1}{48}\int_a^r \frac{1}{x}\lambda(x)\,dx + C_1\right] + r^2\left[-\frac{1}{16}\int_a^r x\lambda(x)\,dx + C_2\right]$$
$$+ \frac{1}{16}\int_a^r x^3\lambda(x)\,dx + C_3 + \frac{1}{r^2}\left[-\frac{1}{48}\int_a^r x^5\lambda(x)\,dx + C_4\right], \tag{A 8}$$

where $C_1, \ldots, C_4$ are integration constants to be determined by the boundary conditions.

From (13) we obtain

$$\langle r_r^{(2)}\rangle_{r=A} = 0, \quad \langle v_\theta^{(2)}\rangle_{r=A} = \kappa\sin 2\theta, \tag{A 9}$$

where

$$\kappa = -\frac{U_0^2}{4\omega}\left[\frac{\omega}{\nu}r\,\mathrm{Re}\,(J+K+M+N) + 2\frac{a^2}{r^3}\,\mathrm{Im}\,(E+G) - \frac{2}{r}\,\mathrm{Im}\,(K+N)\right]_{r=A}.$$

This leads to

$$\left.\begin{aligned} C_1 &= \frac{g(A,a)(A^2-a^2) - 2h(A,a)(A^2+a^2)}{2A^2(A^2-a^2)^3}, \\ C_2 &= \frac{g(A,a) - 4(A^6-a^6)C_1}{2(A^4-a^4)}, \\ C_3 &= -3a^4C_1 - 2a^2C_2, \quad C_4 = 2a^6C_1 + a^4C_2. \end{aligned}\right\} \tag{A 10}$$

Here

$$\left.\begin{aligned} g(A,a) &= \kappa A^3 - \frac{A^6}{12}\int_a^A \frac{1}{x}\lambda(x)\,dx + \frac{A^4}{8}\int_a^A x\lambda(x)\,dx - \frac{1}{24}\int_a^A x^5\lambda(x)\,dx, \\ h(A,a) &= -\frac{1}{48}\left(A^6\int_a^A \frac{1}{x}\lambda(x)\,dx - \int_a^A x^5\lambda(x)\,dx\right) \\ &\quad + \frac{A^2}{16}\left(A^2\int_a^A x\lambda(x)\,dx - \int_a^A x^3\lambda(x)\,dx\right). \end{aligned}\right\} \quad \text{(A 11)}$$

Stokes drift

Inserting the linearized solution (A 3) in the correction term for the stream function

$$C(r,\theta) = -\tfrac{1}{2}\langle \mathbf{v}_u \times \int \mathbf{v}_u\,dt\rangle,$$

we obtain for the two-cylinder case

$$\begin{aligned} C(r,\theta) = -\frac{U_0^2}{2\omega}\sin 2\theta\,\mathrm{Im}\Big\{ & D^*K + JK^* + \frac{a^2}{r^2}(DE^* + J^*E) \\ & + (F-M)\left[\frac{a^2}{r^2}(E^*+G^*) - K^* - N^*\right] + (D-J)\left(\frac{a^2}{r^2}G^* - N^*\right)\Big\}. \end{aligned} \quad \text{(A 12)}$$

The stream function for the Lagrangian velocity is thus

$$\psi_s^L = [g(r) + C_r(r)]\sin 2\theta, \quad \text{(A 13)}$$

where the definition of $C_r(r)$ is obvious.

A necessary condition for a non-zero Stokes drift is that the phase of the oscillations be a function of the space co-ordinates. For, writing

$$\mathbf{v}_u = \mathbf{e}_r v_r \cos(\omega t + \phi_r(r,\theta)) + \mathbf{e}_\theta v_\theta \cos(\omega t + \phi_\theta(r,\theta)),$$

where v_r and v_θ are the amplitudes of the r and θ components of the velocity and ϕ_r and ϕ_θ describe the space variations of the phase, we find, on inserting this in

$$\Delta\mathbf{v}_s = \langle(\int \mathbf{v}_u\,dt).\nabla v_u\rangle,$$

that only terms in which the derivatives of ϕ_r and ϕ_θ enter give a non-zero contribution.

REFERENCES

Bertelsen, A. 1971 Thesis (in Norwegian), Department of Physics, University of Bergen, Norway.

Davidson, B. J. & Riley, N. 1972 *J. Fluid Mech.* **53**, 287–303.

Fjæra, O. 1970 Thesis (in Norwegian), Department of Applied Mathematics, University of Bergen, Norway.

Holtsmark, J., Johnsen, I., Sikkeland, T. & Skavlem, S. 1954 *J. Acoust. Soc. Am.* **26**, 26–39.

Nyborg, W. L. 1965 *Physical Acoustics*, vol. 2, part B, pp. 265–331. Academic.

Olsen, T. 1955 Thesis (in Norwegian), Department of Physics, University of Oslo, Norway.

Olsen, T. 1956 *J. Acoust. Soc. Am.* **28**, 313.

RANEY, W. P., CORELLI, J. C. & WESTERVELT, J. P. 1954 *J. Acoust. Soc. Am.* **26**, 1006–1014.

RAYLEIGH, LORD 1945 *The Theory of Sound*, vol. 2, pp. 333ff. Dover.

RILEY, N. 1965 *Mathematika*, **12**, 161–175.

RILEY, N. 1967 *J. Inst. Maths. Applics.* **3**, 419–434.

SCHLICHTING, H. 1932 *Phys. Z.* **33**, 327–335.

SKAVLEM, S. & TJØTTA, S. 1955 *J. Acoust. Soc. Am.* **27**, 26–33.

SKOGEN, N. 1951 *Kgl. Norske Vidensk. Selskab Forh.* **24**, 68–71.

STOKES, G. G. 1847 On the theory of oscillatory waves. *Trans. Camb. Phil. Soc.* **8**, 441–455. (Reprinted in *Mathematical and Physical Papers*, vol. 1, pp. 314–326. Cambridge University Press.)

STUART, J. T. 1966 *J. Fluid Mech.* **24**, 673–687.

SVARDAL, A. 1965 *Dept. Appl. Math., University of Bergen, Norway, Rep.* no. 7.

WANG, C.-Y. 1968 *J. Fluid Mech.* **32**, 55–68.

WESTERVELT, P. J. 1953 *J. Acoust. Soc. Am.* **25**, 60–68.

WILLIAMS, R. E. & HUSSEY, R. G. 1972 *Phys. Fluids*, **15**, 2083.

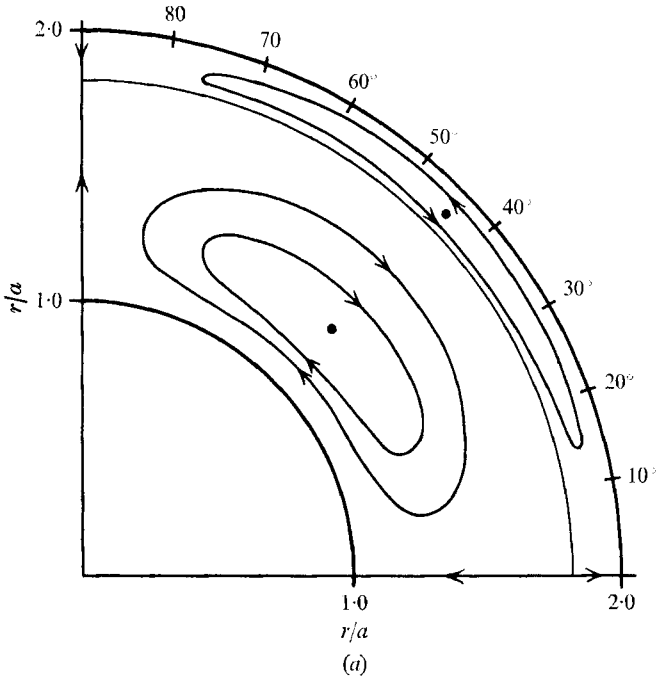

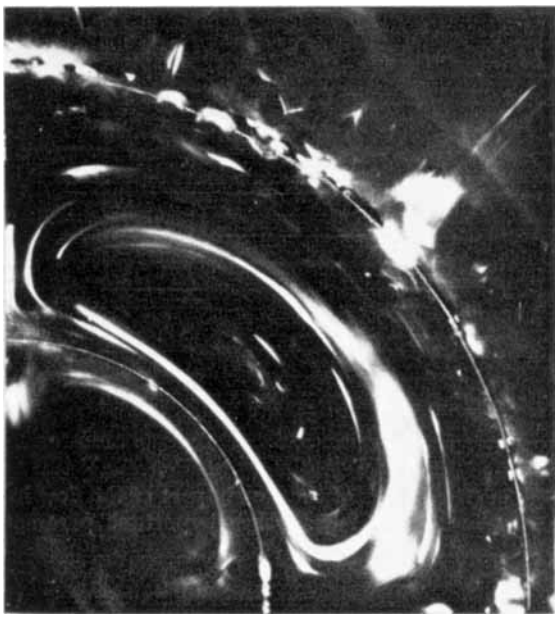

(*b*)

FIGURE 4. (*a*) Lagrangian streamlines of the steady part of the flow in one quadrant from the two-cylinder theory for $A/a = 2{\cdot}0$. Other important parameters as in table 1. (*b*) Corresponding experimental results.

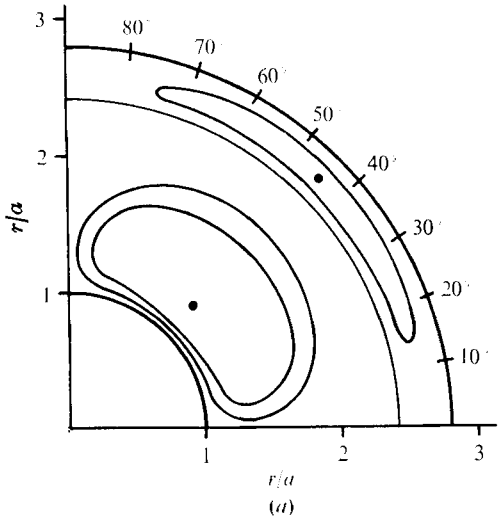

(*b*)

FIGURE 5. (*a*) Lagrangian streamlines of the steady part of the flow in one quadrant from the two-cylinder theory for $A/a = 2{\cdot}82$. Other important parameters as in table 1. (*b*) Corresponding experimental results.

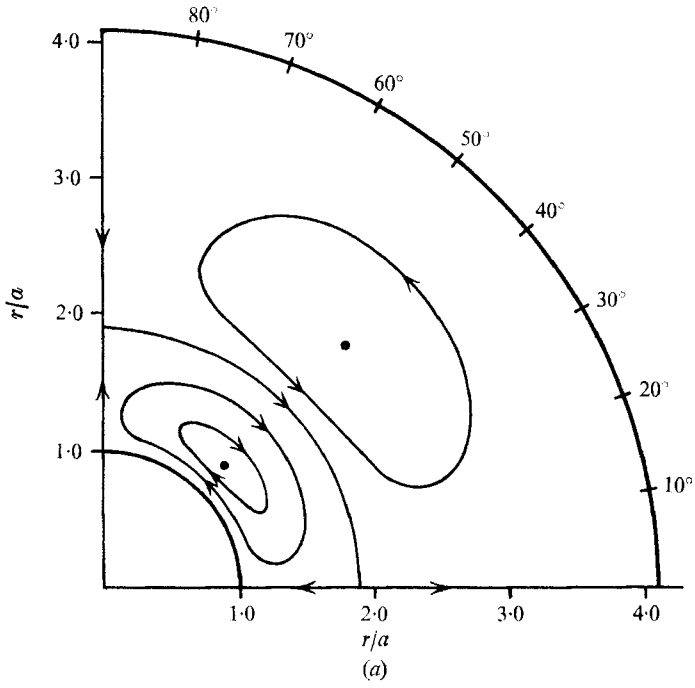

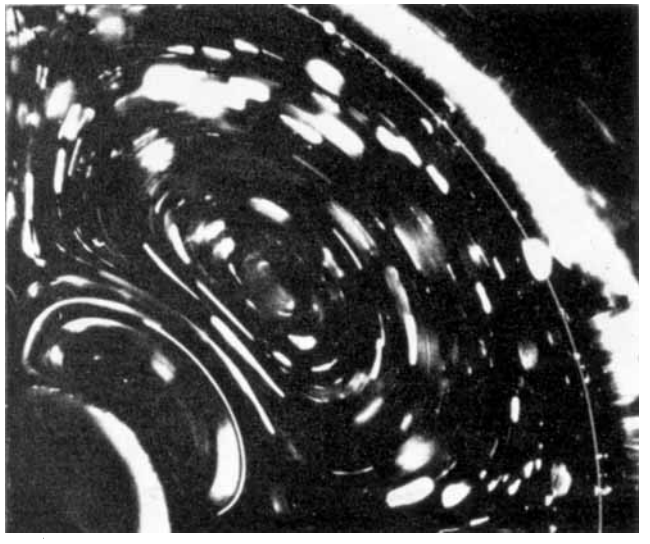

(b)

FIGURE 6. (*a*) Lagrangian streamlines of the steady part of the flow in one quadrant from the two-cylinder theory for $A/a = 4{\cdot}08$. Other important parameters as in table 1. (*b*) Corresponding experimental results.

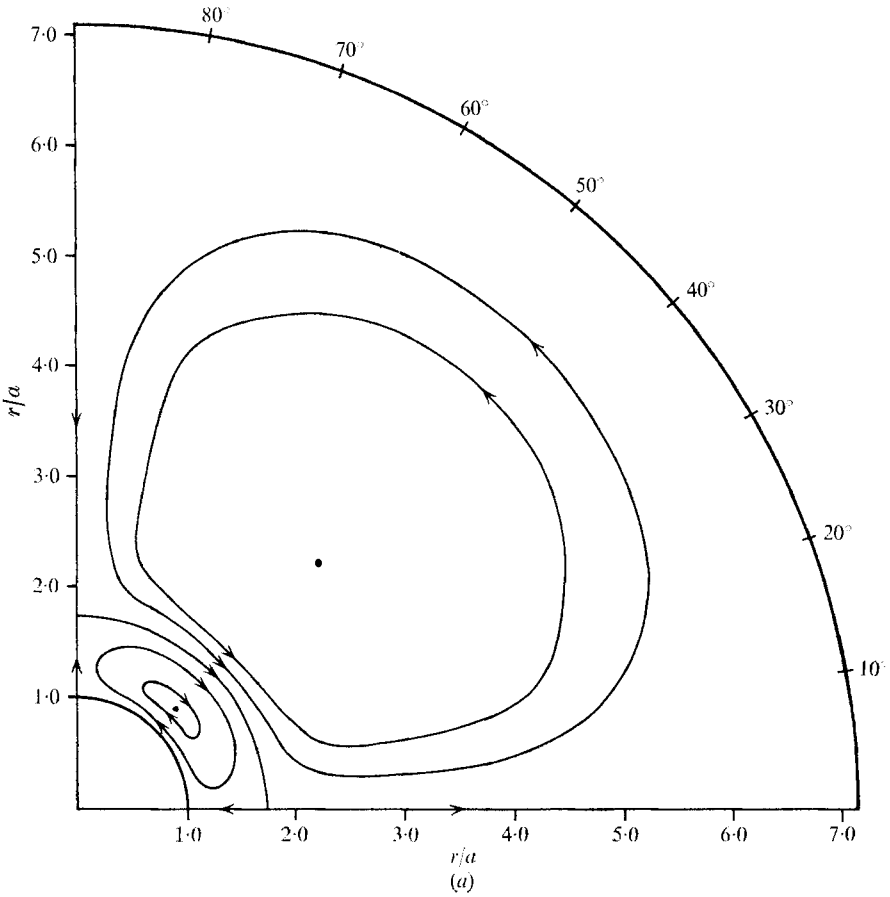

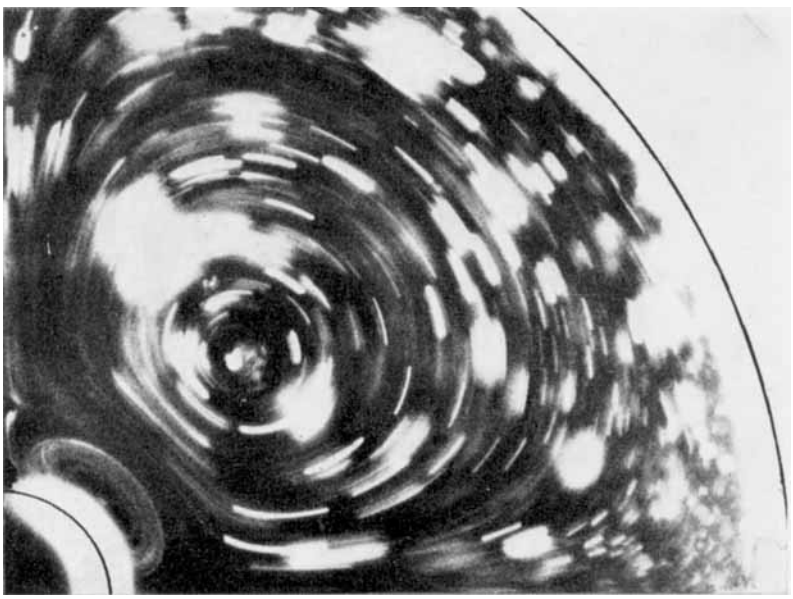

(*b*)

FIGURE 7. (*a*) Lagrangian streamlines of the steady part of the flow in one quadrant from the two-cylinder theory for $A/a = 7{\cdot}14$. Other important parameters as in table 1. (*b*) Corresponding experimental results.

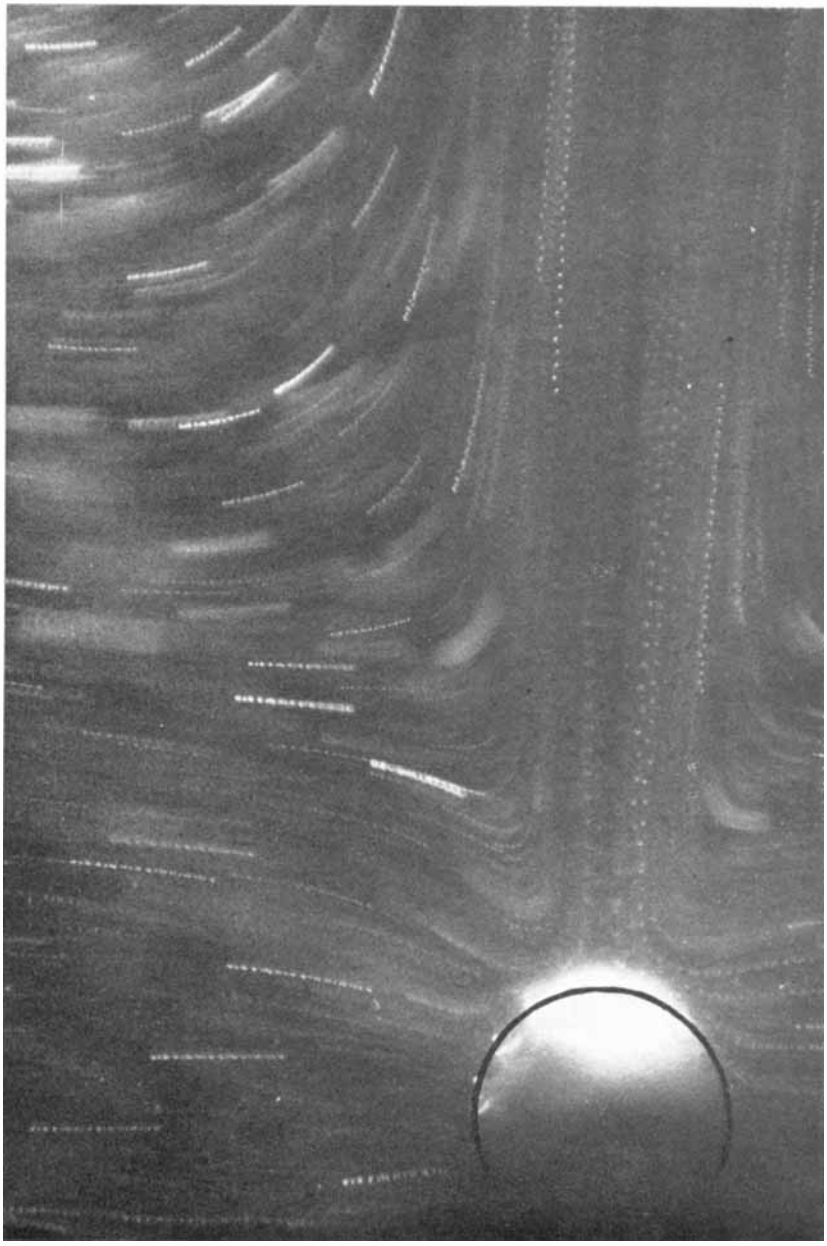

FIGURE 13. Main features of the steady part of the flow observed at $R_s \approx 90$, $a \approx 0{\cdot}15$ cm, $\omega \approx 2\pi\ 350\ \mathrm{s}^{-1}$, $\nu \approx 0{\cdot}0038\ \mathrm{cm}^2/\mathrm{s}$, $U_0 \approx 27{\cdot}5\ \mathrm{cm}/\mathrm{s}$, $A/a \approx 20$.